

Physicochemical Studies on Tomato Bushy Stunt Virus Variants

ANTONIO D. MOLINA-GARCIA,¹ STEPHEN E. HARDING,^{1*} and RONALD R. S. FRASER²

¹University of Nottingham, Department of Applied Biochemistry and Food Science, Sutton Bonington LE12 5RD, and

²Institute of Horticultural Research, Littlehampton, West Sussex, England

SYNOPSIS

Tomato bushy stunt virus particles have previously been physically and chemically well characterized. Different strains, however, are known to have different host plants and symptoms, and they can be distinguished serologically. In an attempt to correlate this behavior with physicochemical properties, we have performed a comparative study on isolates of four of the main variants of this virus (Type strain, petunia asteroid mosaic virus, pelargonium leaf curl virus, and carnation Italian ringspot virus) with regard to sedimentation velocity characteristics, translational diffusivity (from quasi-elastic light scattering measurements), and molecular weight (from both low-speed sedimentation equilibrium and the Svedberg equation).

It is demonstrated that there are no clear differences between the four strains, particularly insofar as their sedimentation characteristics (both velocity and low-speed equilibrium). There is some suggestion from diffusion measurements that the Type strain virus particles may have a higher mass, although the presence of some aggregation phenomena may provide an alternative explanation for the diffusion data.

INTRODUCTION

Tomato bushy stunt virus (TBSV : R/1 : 1.5/17 : S/S : S/*) is a small quasi-spherical plant virus causing disease in numerous dicotyledons. Since it was first described,¹⁻³ it has been well characterized, both physically (see, e.g., Refs. 2-16) and chemically (e.g., Refs. 17 and 18). TBSV particles are approximately 30 nm in diameter, with the protein shell containing 90 morphological units each composed of two protein molecules ($M_r \sim 38,000$) that are identical in their sequence but apparently not in their structure.¹⁹ Each morphological unit is located in the twofold axis of a $T = 3$ icosahedral surface lattice.¹⁴ There is evidence of a minor protein of $M_r \sim 28,000$, of which 12 units are believed to be included in this assembly,¹³ although recent evidence has suggested this is a product of proteolysis.²⁰ One piece of linear positive-sense single-stranded RNA counts for 16-17% of the particle weight.¹⁷

Several strains of this virus have been described; Type strain (Type-TBSV),¹ pelargonium leaf curl virus (PLCV),⁸ petunia asteroid mosaic virus (PAMV),²¹ and carnation Italian ringspot virus (CIRV)²² are the principal variants. Different host plants, symptoms,^{8,20,23} and significant serological differences have been found²¹⁻²⁵ (for example, the different strains can be distinguished immunoelectrophoretically). Although the amino acid sequence of the coat protein is not known for all the variants, the amino acid composition is known to differ from strain to strain.^{17,18,26,27}

The present study is an attempt to correlate the reported differences in biological properties of the principle strains of TBSV with physicochemical properties, with regard to sedimentation velocity, translational diffusivity, and molecular size.

MATERIALS AND METHODS

Viruses

Isolates of the four strains of TBSV used in this work (Type strain, carnation Italian ringspot virus,

© 1990 John Wiley & Sons, Inc.

CCC 0006-3525/90/10-111443-10 \$04.00

Biopolymers, Vol. 29, 1443-1452 (1990)

* To whom correspondence should be addressed.

petunia asteroid mosaic virus and pelargonium leaf curl virus) were obtained from Dr. A. Brunt (Glasshouse Crops Research Institute, Littlehampton, UK). They were grown by inoculation in young plants of *Nicotiana clevelandii*,²⁰ which were harvested 2–3 weeks later.³ Plants were used immediately or else were frozen at -20°C , conditions at which TBSV particles were found to be stable (as judged by absorption spectroscopy and sedimentation velocity).

Purified TBSV was obtained using the procedure of Hollings et al.^{28,23} Virus preparations were then further purified by density sucrose gradient centrifugation.²⁹

Transmission electron microscopy was performed on the samples at various stages of purification in order to check for structural integrity and the absence of contaminants. All preparations contained isometric particles at high concentration. Homogeneity of preparations was checked also by sedimentation velocity (Figure 1) and quasi-elastic light scattering (QLS).

Prior to hydrodynamic characterization, all samples were dialyzed extensively against a phosphate buffer (I 0.10, pH 6.2) with the relevant proportions of Na_2HPO_4 , KH_2PO_4 , and NaCl used according to Green.³⁰

Translational Diffusion Coefficient Measurements: QLS

QLS measurements were performed using Malvern 4700 light scattering equipment equipped with a Siemens 40 mW He/Ne laser (wavelength (λ) = 632.8 nm). The beam from the laser was focused on to the center of a 1×1 cm cuvette. The cuvette was placed at the center of a goniometer so that the scattering angle could be varied from 5° to 90° . Like turnip yellow mosaic virus,³¹ measured diffusion coefficients showed no trend with changing angle, so that an angle of 90° was normally utilized to minimize effects of dust.³² Scattered light was collected by an EMI photomultiplier via a well-collimated pinhole (aperture $100 \mu\text{m}$) and via an Amplifier-Discriminator to a 64-channel Malvern Autocorrector (K7032-OS). The digital correlator output was stored on floppy disks and then sent via an Olivetti M24 microcomputer to the University of Cambridge IBM 3081/B computer (via the JANET link) for processing. The routine used produced an accurate plot of $\log[g^2(t) - 1]$ vs time t , where $g^2(t)$ is the normalized intensity correlation function. The z -average (apparent translational) diffusion coefficients were obtained from the limiting slope³³ of this plot. The routine produced the best least-squares fit

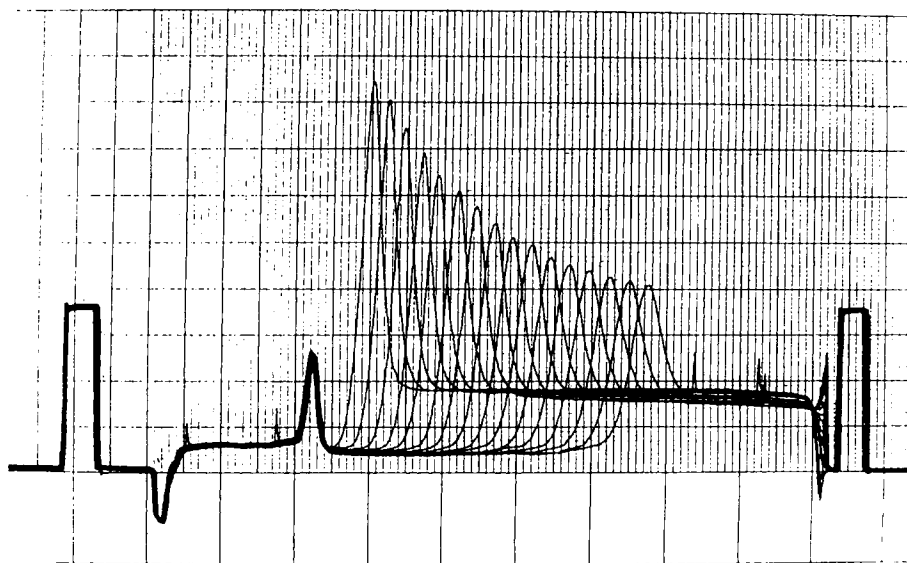


Figure 1 Sedimentation velocity diagram for a solution of Type-TBSV obtained using knife-edge Schlieren scanning optics. Rotor speed = 11,000 rev/min, temperature = 20.0°C . Loading concentration 5.5 mg/mL. Direction of sedimentation from left to right. Scan interval = 6 min. [The raised baseline in advance of the Schlieren peak is a feature of the knife edge used with the Centriscan (as opposed to the phase plate used in other types of analytical ultracentrifuge). With the knife edge system, baseline = Σ (optical Schlieren baseline + turbidity)].

to a linear, quadratic, or cubic polynomial, and a guide to the best fit was provided by the ϵ function³⁴ (this is essentially a sum of squares of residuals function normalized for the number of degrees of freedom). The routine also calculated the "polydispersity factor," namely, the z -averaged normalized variance of the diffusion coefficient distribution (see, e.g., Ref. 33).

Translational diffusion coefficients D_c at a finite concentration c , and an absolute temperature T (in this study 298.15 K), were normalized to standard conditions (water as solvent at 20°C) according to the usual formula (see, e.g., Ref. 31).

$$D_{c(20,w)} = \frac{293.15}{T} \cdot \frac{\eta_{T,b}}{\eta_{20,w}} \cdot D_{c(T,b)}$$

where $\eta_{T,b}$ is the solvent viscosity at a temperature T and $\eta_{20,w}$ the viscosity of water at 20°C.

In all that follows we use the symbol D_c instead of $D_{c(20,w)}$, and D as the value of the D_c extrapolated to infinite dilution.

Sample times of 3 μ s were normally used. No dependence of diffusion coefficient with sample time was observed, so a correction to zero sample time was not found necessary. Experimental duration times ranging from 1 to 6 min were chosen depending on each particular experiment concentration, so as to ensure a high number of counts ($\sim 10^8$) to be stored in the autocorrelator channels.

Cleaning of Cells and Clarification of Solutions for QLS

The cleaning and clarification procedures were essentially as described by Godfrey et al.³² Each cell was repeatedly flushed with ultrafiltered water by using a filling apparatus similar to that described by Sanders and Cannell,³⁵ and then dried with ultrafiltered air. Virus solution was then introduced into the cell through a Millipore (type HA, 0.45- μ m pore size) filter fitted to a hypodermic needle.

Water in the index-matching bath was filtered also, first through a coarse filter and then through a 0.45- μ m Millipore filter HA type for 15 min. The contribution of particles in suspension in this bath or in filtered deionized water in the sample cell was shown to be negligible.

Concentration Measurements

Concentrations of TBSV solutions were determined spectrophotometrically using an Ultrospec 4050 (LKB Instruments, Bromma, Sweden) controlled

from a BBC microcomputer, with a 1-mm optical path-length quartz cell. An extinction coefficient of 4.5 mL \cdot mg⁻¹ \cdot cm⁻¹ at 260 nm¹⁰ was used, after graphically correcting absorbance for light scattering. Concentrations for the diffusion measurements were measured after filtration.

Sedimentation Coefficient Measurements

Sedimentation velocity experiments were performed using an MSE Centriscan analytical ultracentrifuge equipped with scanning absorption and Schlieren optics and a monochromator. Measurements were performed at temperatures between 20.0–23.0°C and at a speed of 11,000 rev/min. Schlieren measurements were at a wavelength of 546 nm, absorption measurements near 280 nm. Single symmetrical boundaries (Figure 1) were always observed (although such symmetry is not in itself proof of homogeneity—see, e.g., Ref. 36).

Eight to twelve scans were used in determining each value of the sedimentation coefficient at a particular concentration c (corrected for radial dilution). The sedimentation data were captured using a Cherry digitizing Tablet interfaced to an Apple IIE computer, which evaluated the sedimentation coefficient and the radial dilution correction factor for concentration.

All sedimentation coefficients, at finite concentrations c were corrected to standard conditions (water as solvent at 20°C) in the usual way:

$$s_{c(20,w)} = \frac{(1 - \bar{v}\rho)_{20,w}}{(1 - \bar{v}\rho)_{T,b}} \cdot \frac{\eta_{T,b}}{\eta_{20,w}} \cdot s_{c(T,b)}$$

\bar{v} being the partial specific volume and ρ the solution density. A partial specific volume for TBSV particles of 0.712 mL/g³⁷ was employed. In all that follows the symbol s_c will be used in place of $s_{c(20,w)}$, and s corresponds to the value at infinite dilution.

Use of solution densities for each concentration is rather difficult, tedious, and wasteful of material, and so we follow the common procedure of using solvent densities. This has no effect on the value of s_c extrapolated to infinite dilution (s) (see, e.g., Ref. 31).

Sedimentation Equilibrium Measurements

Sedimentation equilibrium experiments were performed using a Beckman Model E analytical ultracentrifuge equipped with Rayleigh interferometric optics and an RTIC temperature-measuring system (set for 25.0°C).

Although the procedure for the “low” or “intermediate” speed³⁸ was followed, because of the very high mass of TBSV even at very low speeds (nominally 1967 rev/min), near-depletion conditions were obtained, with unavoidable loss of optical registration of the fringes near the cell base (Figure 2). Nonetheless, the meniscus concentration remained measurable and was obtained by mathematical manipulation of the fringe data.³⁸ The heavy “rotor J” was used to minimize problems of instability at the low speeds used.

Data from the Rayleigh interference patterns were captured off-line on an LKB Ultrosan XL [two-dimensional (2D) scanner], interfaced to a PC. Fringe concentration vs radial displacement plots were obtained using the UCSD PASCAL routine “ANALYSE2.” This is essentially the same as the routine ANALYSER described earlier^{39,40} but modified for the 2D scanner (see Ref. 41). This data was then transferred via the joint UK Computer network (JANET) for full analysis on the mainframe IBM 3081/B at Cambridge.

Whole-cell weight average relative molecular masses, M_w^0 were obtained by using the limiting value at the cell base of a directly determinable point average M^* .³⁸ An independent estimate for the initial concentration was not required. To minimize the effects of thermodynamic nonideality, very low concentrations were employed (~ 0.2 mg/mL) in 30-mm optical path-length cells.

Transmission Electron Microscopy

Transmission electron microscopy (Figure 3) was used to check for the purity and integrity of the virus strains used for hydrodynamic characterization. Samples were checked using electron microscopy

periodically during the course of the hydrodynamic measurements. A Corinth 275 transmission electron microscope was used, and two different types of negative staining procedure were employed; in one, undiluted or several-fold diluted (with the phosphate buffer described) samples were wetted with 0.05% bacitracine solution, negatively stained with 2% methylamine tungstate, and placed on top of carbon-coated copper grids. In the other, preparations were negatively stained using uranyl acetate after fixation of particles by glutaraldehyde vapors for ~ 1 min and then placed on the same type of grids.

RESULTS AND DISCUSSION

Homogeneity

All samples produced a single symmetric Schlieren boundary peak (Figure 1) when checked by sedimentation velocity and did not show any other type of particle when checked by transmission electron microscopy (Figure 3). Also, the “polydispersity factor” obtained from QLS measurements was relatively small in every case (within the range 0.0–0.2), indicating monodispersity, as did the crude estimate of a diffusion coefficient distribution using the PCS manufacturer’s (Malvern Instruments, UK) own software (data not shown).

Sedimentation Coefficient Measurements

Values for the sedimentation coefficients (corrected to water and 20°C, and extrapolated to “infinite dilution”) for each of the strains studied are given in Table I, and are very similar (within the range $(128\text{--}132) \times 10^{-13}$ s). The dependence of the sedimentation coefficient with concentration (corrected for

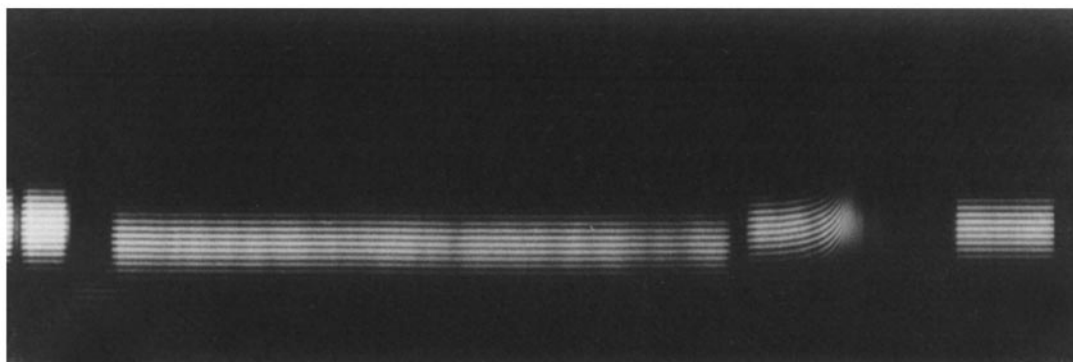


Figure 2 Rayleigh interference fringe profiles from PLCV at sedimentation equilibrium. Rotor speed = 1,957 rev/min, temperature = 25.0°C. Initial loading concentration $C^0 \sim 0.2$ mg/mL. Solvent: standard phosphate chloride, pH = 6.2, I = 0.10.

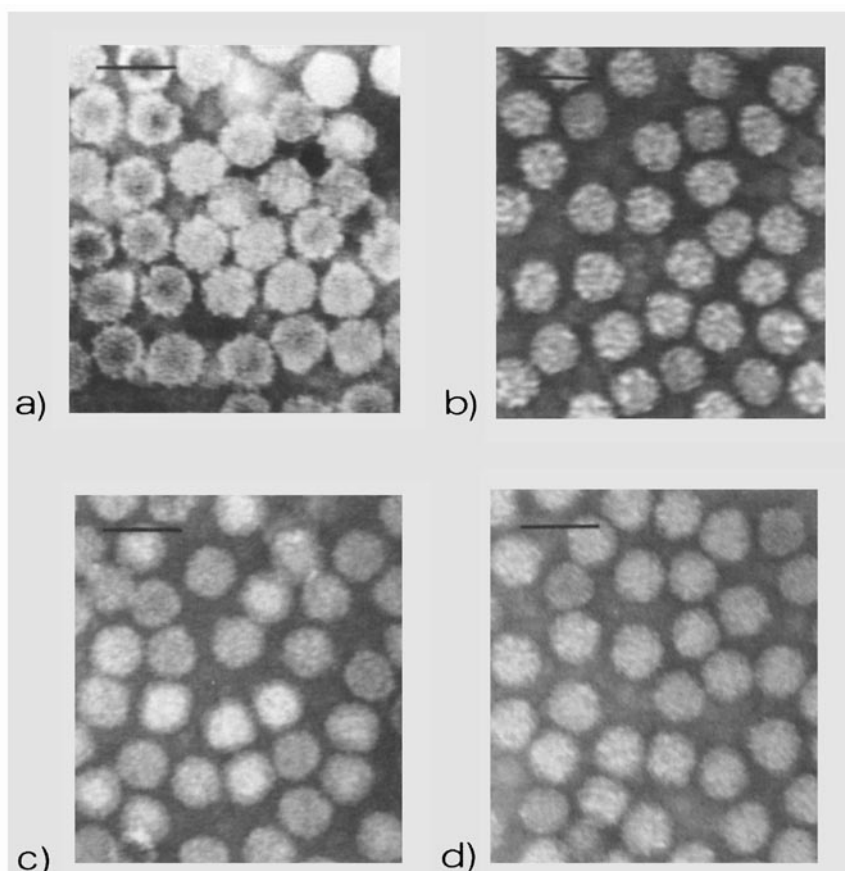


Figure 3 Electron microscopy of TBSV particles negatively stained using 1% uranyl acetate. The bar corresponds to 50 nm. (a) PAMV, (b) PLCV, (c) CIRV, and (d) Type-TBSV virus.

for radial dilution effects) was relatively small for all four strains (Figure 4).

Literature values for sedimentation coefficients for particles of the strains of TBSV considered in this study are in the range $(131\text{--}146) \times 10^{-13}$ s.^{4,8,10,11,22,42,43} It is worth noting that the particular value for Type-TBSV from the present study, $(132 \pm 2) \times 10^{-13}$ s, corresponds with the value of 132×10^{-13} s given by Lauffer and Stanley⁴² and Hollings and Stone.⁸

Diffusion Coefficient Measurements

Linear plots of the normalized autocorrelation function vs time were obtained for all four TBSV variants. Although diffusion coefficients are generally less sensitive to concentration changes than sedimentation coefficients (due to opposing effects of the concentration dependence of the frictional coefficient and thermodynamic nonideality—see, e.g., Ref. 44) an extrapolation to zero concentration

Table I Physical Parameters of TBSV Variants^a

Strains	$10^{13} \times s$ (s)	$10^7 \times D$ ($\text{cm}^2 \text{s}^{-1}$)	PF	$10^{-6} \times M_r$ (s, D)	$10^{-6} \times M_r$ (sed. eq.)	r_H (nm)
PAMV	128 ± 2	1.22 ± 0.02	0.05 ± 0.04	8.9 ± 0.3	9.7 ± 1.0	17.3 ± 0.3
PLCV	127 ± 2	1.23 ± 0.06	0.035 ± 0.006	8.8 ± 0.6	9.7 ± 1.0	17.1 ± 0.8
CIRV	128 ± 2	1.14 ± 0.02	0.09 ± 0.03	9.6 ± 0.2	8.5 ± 1.0	18.5 ± 0.3
Type-TBSV	132 ± 2	1.05 ± 0.03	0.15 ± 0.04	10.7 ± 0.4	9.5 ± 1.0	20.1 ± 0.6

^a s, D : infinite dilution sedimentation and z -average translational diffusion coefficients, respectively, corrected to water as solvent at 20.0°C. PF: polydispersity factor. M_r (s, D): weight average molecular weight determined from sedimentation and diffusion coefficients. M_r (sed. eq.): weight average molecular weight determined by low-speed sedimentation equilibrium. r_H : "Stokes radius" obtained from the diffusion coefficient.

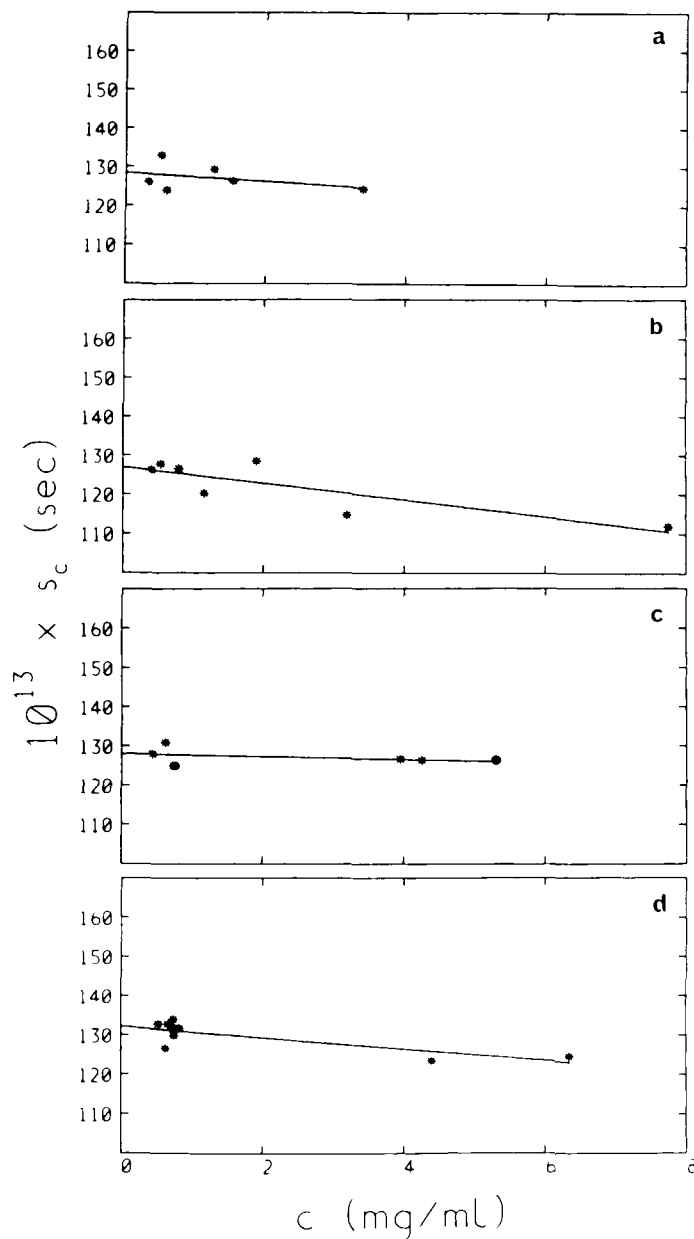


Figure 4 Sedimentation coefficient vs concentration plots for TBSV particles. (a) PAMV, (b) PLCV, (c) CIRV, and (d) Type-TBSV. Solvent as in Figure 2.

was still deemed necessary (Figure 5). Table I gives the infinite dilution values of the diffusion coefficients obtained by linear least-squares regression to these plots. Two of the variants (PAMV and PLCV) appear similar $D = (1.22, 1.23) \times 10^{-7} \text{ cm}^2 \text{ s}^{-1}$, respectively, although the value for the CIRV and Type variants appears somewhat lower: $(1.14 \pm 0.02) \times 10^{-7}$ and $(1.05 \pm 0.03) \times 10^{-7} \text{ cm}^2 \text{ s}^{-1}$, respectively. Using QLS, Camerini-Otero et al.⁴⁵ have obtained for the translation diffusion coefficient

(D) of TBSV a value of $(1.246 \pm 0.012) \times 10^{-7} \text{ cm}^2 \text{ s}^{-1}$, which appears consistent with our results for PAMV and PLCV variants. Closer to our value for the CIRV and "type" variants is a much earlier value of 1.15×10^{-7} given by Neurath and Cooper⁴⁶ for the Type variant, using "classical" boundary spreading in the ultracentrifuge.

The low value for Type-TBSV could be due to a genuine size difference. A more likely explanation, however, is that it is symptomatic of the presence

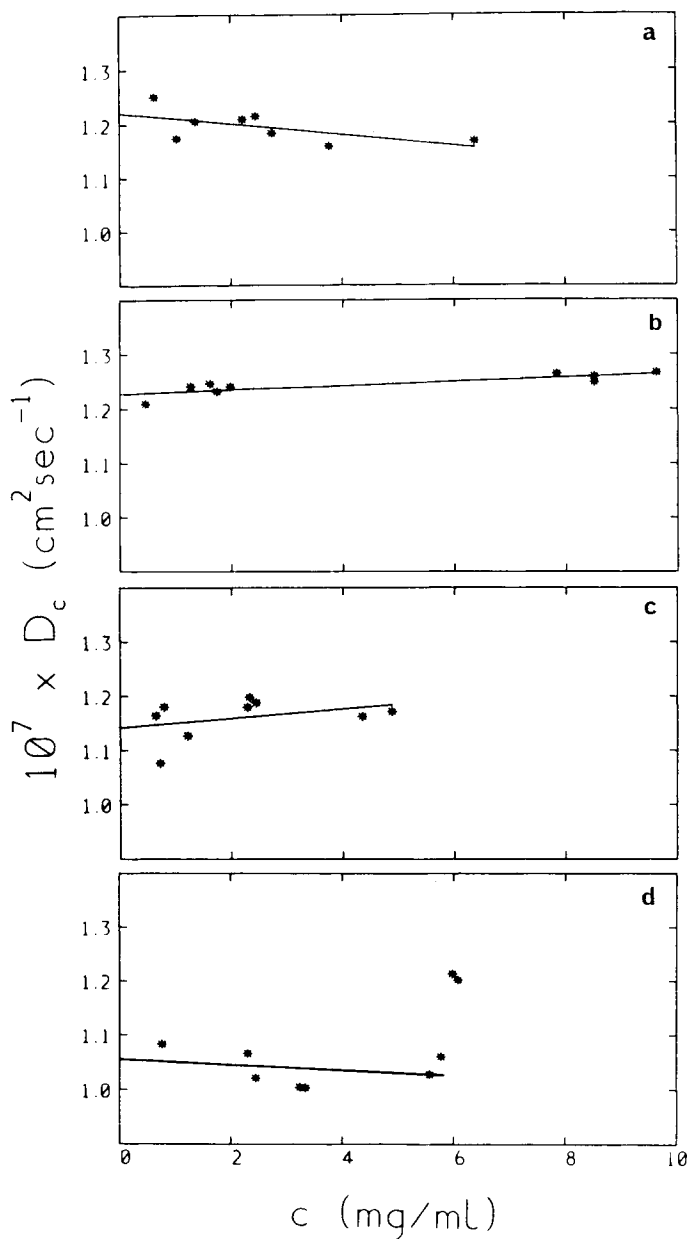


Figure 5 Translational diffusion coefficient vs concentration plots for TBSV particles. (a) PAMV, (b) PLCV, (c) CIRV, and (d) Type-TBSV. Solvent as in Figure 2. In (d) the highest two concentration points are not used (more than two standard deviations away from regression line).

of aggregates. This view is supported by the greater noise in the data (Figure 5d), although aggregates were not detected by sedimentation velocity.

Molecular Weight Determinations

We have obtained the (weight average) molecular weight for the TBSV strains in two ways (Table I): (1) from the Svedberg equation by combining sed-

imentation coefficient with diffusion coefficient data, and (2) by low-speed sedimentation equilibrium using the M^* function extrapolated to the cell base (Figure 6). We have made the assumption throughout (due to scarcity of material) that the partial specific volume \bar{v} is the same for all four strains. This would appear reasonable unless there were significant differences in the protein/nucleic acid ratio for the different strains. Despite the larger errors

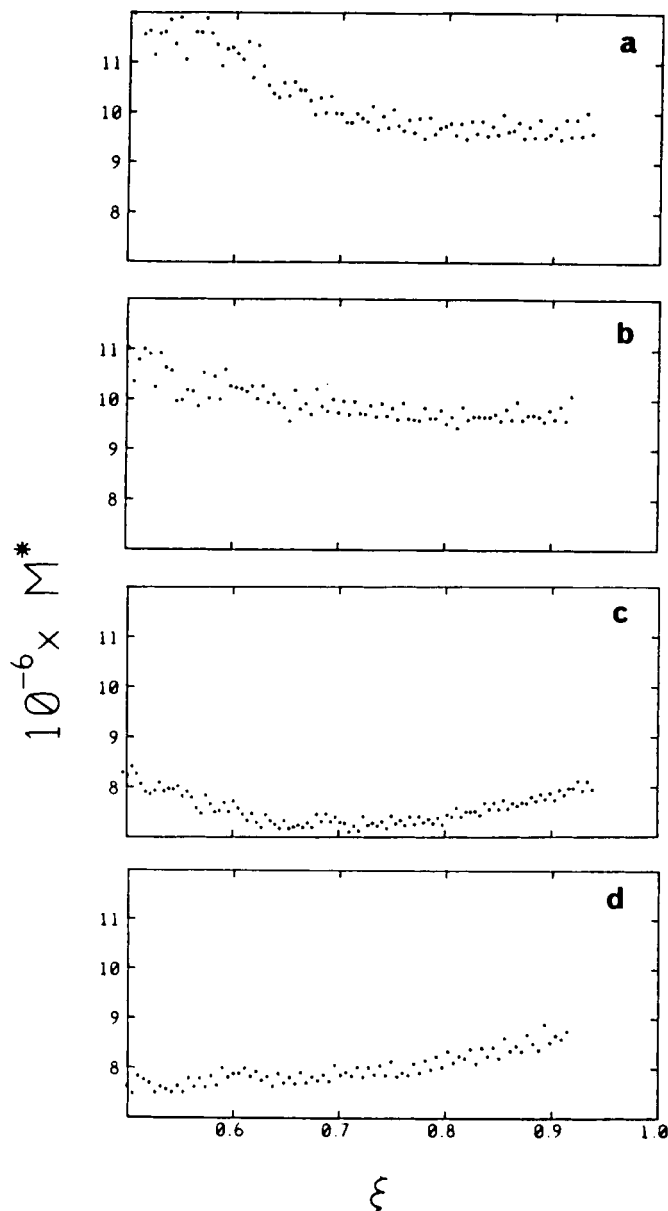


Figure 6 M^* vs ξ plots for TBS virus particles for (a) PAMV, (b) PLCV, (c) CIRV, and (d) Type-TBSV. Loading concentrations ≈ 0.2 mg/mL. Rotor speeds = 1967 rev/min temperature = 25.0°C. Solvent as in Figure 2. $\xi = (r^2 - a^2)/(b^2 - a^2)$, r being the radial displacement, and a and b the corresponding values for the cell meniscus and base, respectively. $M_w^0 = M^*(\xi \rightarrow 1)$. Due to the errors in measuring fringe increments at low values of ξ and errors in selection of the meniscus concentrations for particles in this size range, no significance is attached to the dependence of M^* on ξ (Ref 39).

associated with the latter procedure (almost the top M_r limit for sedimentation equilibrium), the results are in good agreement with those from the Svedberg equation and suggest molecular weights for the strains of TBSV within the range of 8.5–10 million. The one exception is for the Type strain, where the results from the Svedberg equation (only) suggest a larger weight average—due to the slightly higher

sedimentation coefficient and lower translational diffusion coefficient. It could be inferred, on the basis of the Svedberg equation, that the Type strain particles would be generally larger. Alternatively as noted above, the presence of small amounts of aggregates would cause lower diffusion coefficient values (and hence higher Svedberg equation molecular weights). Such aggregates, if present, would be lost

from optical registration at the cell base in sedimentation equilibrium and would not bias the results to the same degree. The results thus found would therefore appear to demonstrate (1) a larger size or a greater tendency of one strain (Type-TBSV) to form aggregates, and (2) the advantages of using sedimentation equilibrium as opposed to a method involving a light scattering measurement on systems that are potentially aggregating.

Values given by earlier workers for molecular weights of TBSV range from $7.1\text{--}13.0 \times 10^6$.^{4,11,37,42,45-52} These values have been obtained, however, by a wide variety of methods and in conditions often very different of those of this work (e.g., prepared for electron microscopy; see Ref. 48). Nevertheless, a value of $\sim 10.6 \times 10^6$ for M_r (obtained by Neurath and Cooper⁴⁶ using the Svedberg equation from their diffusion coefficient—classical boundary spreading in the ultracentrifuge—and a sedimentation coefficient of $\sim 132 \times 10^{-13}$ s of Lauffer and Stanley⁴² appears in good agreement with the value obtained from the Svedberg equation for the Type strain.

Earlier reported hydrodynamic radii for TBSV also show some variability (from 13.5 to 17.2 nm).^{2,4-8,11,16,28,42,45,52-55,56} Apart from the value of (17.2 ± 2) nm obtained by Camerini-Otero et al.⁴⁵ for PAMV using photon correlation spectroscopy, values are generally lower than those obtained in this study. It must be noted that most of the other earlier values have been obtained by electron-microscopical or other methods in which the radius measured would not generally include the contribution from particle solvation (e.g., Refs. 5, 7, 8, 28, 42, 53-55).

TBSV and related viruses are known to undergo a size change controlled by pH and Ca^{2+} ions (see, e.g., Refs. 57-60). In the buffer employed in this work the TBSV variants would therefore be in a relatively "compact" state. As far as we are aware, there has been no report of the effects of pH or the presence of divalent cations on PAMV, PLCV, or CIRV particles. There is also a variety of methods for purification of the particles, and some of these might affect their physical properties to some extent (e.g., see Ref. 61). We would also like to stress that in many of the studies on TBSV there has been no specification of which particular variant is employed. Indeed, the strains themselves (PAMV, PLCV, CIRV, and Type-TBSV) exist in different forms (see, e.g., Ref. 27). This may be an important cause of disagreement as there appears to be as much difference in some properties among TBSV isolates than among different strains.⁶²⁻⁶⁴

Serological tests (namely spur formation in gel-diffusion test and immunoelectrophoresis) have shown that TBSV (a member of the "Tombus" group of viruses) can be divided into several families more or less immunologically related. The PLCV, CIRV, and PAMV "families" are closely related although Type-TBSV appears very different from all the rest in its serological behavior.²⁰ Indeed, differences in the external region of the protein capsid of the viruses could well be responsible for detectable differences in size, solvation, or aggregation behavior in any given condition (manifested by differences in the sedimentation and diffusion coefficients) and different immunological behavior. In this context it has been suggested by Koenig and Gibbs⁶⁵ that some electrophoretic behavioral differences among TBSV strains could be due to size rather than charge differences—a feature not inconsistent with our present observations.

We are grateful for the expert technical assistance of M. S. Ramzan (hydrodynamic measurements), A. Gerwitz (virus particle purification), and M. J. W. Webb, C. M. Clay, and S. Hyman (electron microscopy). We thank Dr. A. J. Rowe (Leicester University) for the use of his extensive electron microscopy facilities and Dr. A. Brunt for kindly providing the virus innoculi employed in this work.

REFERENCES

1. Smith, K. M. (1935) *Nature* (London) **135**, 908-909.
2. Smith, K. M. (1935) *Ann. Appl. Biol.* **22**, 731-741.
3. Bawden, F. C. & Pirie, N. W. (1938) *Br. J. Exp. Pathol.* **19**, 251-263.
4. McFarlane, A. S. & Kekwick, R. A. (1938) *Biochem. J.* **32**, 1607-1613.
5. Carlisle, C. H. & Dornberger, K. (1948) *Acta Cryst.* **1**, 194-196.
6. Leonard, B. R., Jr., Anderegg, J. W., Shulman, S., Kaesberg, P. & Beeman, W. W. (1953) *Biochim. Biophys. Acta* **12**, 499-507.
7. Klug, A. & Caspar, D. L. D. (1960) *Adv. Vir. Res.* **7**, 225-325.
8. Hollings, M. & Stone, O. M. (1965) *Ann. Appl. Biol.* **56**, 87-98.
9. Kupke, D. W. (1966) *Fed. Proc. Fed. Am. Soc. Exp. Biol.* **25**, 990-992.
10. Ambrosino, C., Appiano, A., Rialdi, G., Papa, G., Redolfi, P. & Carrara, M. (1967) *Atti. Accad. Sci. Torino* **101**, 301-303.
11. Kalmankoff, J. & Tremaine, J. H. (1967) *Virology* **33**, 10-16.
12. Harrison, S. C. (1969) *J. Mol. Biol.* **42**, 457-483.
13. Butler, P. J. G. (1970) *J. Mol. Biol.* **52**, 589-593.
14. Finch, J. T., Klug, A. & Leberman, R. (1970) *J. Mol. Biol.* **50**, 215-222.

15. Crowther, R. A. & Amos, L. A. (1971) *Cold Spring Harbor Symp. Quant. Biol.* **36**, 489-494.
16. Martelli, G. P. & Russo, M. (1972) *J. Gen. Virol.* **15**, 193-203.
17. De Fremery, D. & Knight, C. A. (1955) *J. Biol. Chem.* **214**, 559-566.
18. Michelin-Lausarot, P., Ambrosino, C., Steere, R. L. & Reichmann, M. E. (1970) *Virology* **41**, 160-165.
19. Winkler, F. K., Schutt, C. E. & Harrison, S. C. (1977) *Nature (London)* **265**, 509-513.
20. Martelli, G. P., Quacquarelli, A. & Russo, M. (1971) Commonwealth Mycological Institute Association of Applied Biologist Descriptions of Plant Viruses, No. 69.
21. Lovisolo, O. (1957) *Boll. Staz. Patol. Veg. Roma* **14**, 103-119.
22. Hollings, M., Stone, O. M. & Bouttell, G. C. (1970) *Ann. Appl. Biol.* **65**, 299-309.
23. Hollings, M. & Stone, O. M. (1975) *Ann. Appl. Biol.* **80**, 37-48.
24. Bercks, R. & Lovisolo, O. (1965) *Phytopathol. Z.* **52**, 96-101.
25. Martelli, G. P. & Quacquarelli, A. (1966) *Atti Congr. Un. Fitopat. Medit.* **1**, 195-199.
26. Tremaine, J. H. (1970) *Phytopathology* **60**, 454-456.
27. Fraenkel-Conrat, H. (1974) in *Comprehensive Virology*, Fraenkel-Conrat, H. & Wagner, R. R., Eds., Plenum Press, New York, p. 111.
28. Hollings, M. (1962) *Ann. Appl. Biol.* **50**, 189-202.
29. Walkey, D. G. A. (1985) *Applied Plant Virology*, Heineman, London, pp. 119, 292-293.
30. Green, A. A. (1933) *J. Am. Chem. Soc.* **55**, 2331-2336.
31. Harding, S. E. & Johnson, P. (1985) *Biochem. J.* **231**, 549-555.
32. Godfrey, R. E., Johnson, P. & Stanley, C. J. (1982) in *Biomedical Applications of Laser Light Scattering*, Satelle, D. B., Lee, W. I. & Ware, B. R., Eds., Elsevier, Amsterdam, pp. 373-389.
33. Pusey, P. N. (1974) in *Photon Correlation and Light Beating Spectroscopy*, Cummings, H. Z. & Pike, E. R., Eds., Plenum Press, New York, p. 387.
34. Teller, D. C. (1973) *Methods Enzymol.* **27**, 346-441.
35. Sanders, A. H. & Cannel, D. S. (1980) in *Light Scattering in Liquids and Macromolecular Solutions*, Degiorgio, V., Corti, M. & Giglio, M., Eds., Plenum Press, New York, pp. 173-182.
36. Gilbert, G. A. & Gilbert, L. M. (1980) *J. Mol. Biol.* **144**, 405-408.
37. Schachmann, H. K. & Williams, R. C. (1959) in *The Viruses*, Burnet, F. M. & Stanley, W. M., Eds., Academic Press, New York, pp. 223-327.
38. Creeth, J. M. & Harding, S. E. (1982) *J. Biochem. Biophys. Methods* **7**, 25-34.
39. Harding, S. E. & Rowe, A. J. (1987) *Biochem. Soc. Trans.* **15**, 1046-1047.
40. Harding, S. E. & Rowe, A. J. (1988) *Optics Lasers Engin.* **8**, 83-96.
41. Rowe, A. J., Wynne-Jones, S. K., Thomas, D. & S. E. Harding, (1989) SPIE Vol. 1163 Fringe Pattern Analysis, 138-148.
42. Lauffer, M. A. & Stanley, W. M. (1940) *J. Biol. Chem.* **135**, 463-472.
43. Lovisolo, O. (1964) *Atti Congr. Un. Fitopat. Med.* **1**, 574-583.
44. Harding, S. E. & Johnson, P. (1985) *Biochem. J.* **231**, 543-547.
45. Camerini-Otero, R. D., Pusey, P. N., Koppel, D. E., Schaefer, D. W. & Franklin, R. M. (1974) *Biochemistry* **13**, 960-970.
46. Neurath, H. & Cooper, G. R. (1940) *J. Biol. Chem.* **135**, 455-462.
47. Oster, G. (1946) *Science* **103**, 306-308.
48. Williams, R. C. & Backus, R. C. (1949) *J. Am. Chem. Soc.* **71**, 4052-4057.
49. Markham, R. (1953) *Progr. Biophys. Biophys. Chem.* **3**, 61-87.
50. Hersh, R. T. & Schachman, H. K. (1958) *Virology* **6**, 234-243.
51. Weber, K., Rosenbusch, J. & Harrison, S. C. (1970) *Virology* **41**, 763-765.
52. Chauvin, C., Witz, J. & Jacrot, B. (1978) *J. Mol. Biol.* **124**, 641-651.
53. Stanley, W. M. & Anderson, F. (1941) *J. Biol. Chem.* **139**, 325-338.
54. Price, W. C., Williams, R. C. & Wyckoff, R. W. G. (1946) *Arch. Biochem.* **9**, 175-185.
55. Williams, R. C. (1953) *Cold Spring Harbor Symp. Quant. Biol.* **18**, 185-195.
56. Kaesberg, P. (1959) in *Proceedings of the First National Biophysics Conference*, Quastler, H. & Morowitz, H. J., Eds., Yale University Press, New Haven, CT, pp. 244-251.
57. Harrison, S. C. (1980) *Biophys. J.* **32**, 139-153.
58. Harrison, S. C. (1984) in *The Microbe 1984, Part I: Viruses (36th Symposium of the Society for General Microbiology)*, Mahy, B. W. J. & Pattison, J. R., Eds., Cambridge University Press, Cambridge, p. 48.
59. Robinson, I. K. & Harrison, S. C. (1982) *Nature* **297**, 563-568.
60. Kruse, J., Kruse, K. M., Witz, J., Chauvin, C., Jacrot, B. & Tardieu, A. (1982) *J. Mol. Biol.* **162**, 393-417.
61. Hollings, M. (1974) *Acta Hort.* **36**, 23-24.
62. Martelli, G. P. (1981) in *Handbook of Plant Virus Infections and Comparative Diagnosis*, Kurstak, E., Ed., Elsevier/North-Holland Biomedical Press, Amsterdam, pp. 61-90.
63. Koenig, R. & Avgelis, A. (1983) *Phytopathol. Z.* **106**, 349-353.
64. Gallitelli, D., Hull, R. & Koenig, R. (1985) *J. Gen. Virol.* **66**, 1523-1531.
65. Koenig, R. & Gibbs, A. (1986) *J. Gen. Virol.* **67**, 75-82.

Received January 5, 1989

Accepted September 6, 1989